LocAP: Accurate Localization of Existing WiFi Infrastructure

This a draft version of the accepted paper

Abstract

Indoor localization has been studied for nearly two decades fueled by wide interest in indoor navigation, achieving the necessary decimeter-level accuracy. However, there are no real-world deployments of WiFi-based user localization algorithms, primarily because these algorithms are triangulation based and therefore assume the location of the Access Points, their antenna geometries, and deployment orientations in the physical map. In the real world, such detailed knowledge of the location attributes of the Access Point is seldom available, thereby making WiFi localization hard to deploy. In this paper, for the first time, we establish the accuracy requirements for the location attributes of access points to achieve decimeter level user localization accuracy. Surprisingly, these requirements for antenna geometries and deployment orientation are very stringent, requiring millimeter level and sub-10° of accuracy respectively, which is hard to achieve with manual effort. To ease the deployment of real-world WiFi localization, we present LocAP, which is an autonomous system to physically map the environment and accurately locate the attributes of existing infrastructure AP in the physical space down to the required stringent accuracy of 3 mm antenna separation and 3^o deployment orientation median errors, whereas state-of-the-art report 150 mm and 25^o respectively.

1 Introduction

Indoor navigation requires precise indoor maps and accurate user location in these maps. To this end, there are two decades of research on indoor localization using WiFi infrastructure achieving decimeter accurate localization, sufficient for indoor navigation [18, 25, 32, 34, 44–46, 51, 52, 57–61]. Furthermore, Google, Bing, Apple or Open Street Maps provide indoor maps for notable locations like airports, shopping malls [1–4]. In spite of these innovations, we still cannot use our smartphones to navigate in indoor environments such as airports or shopping malls. The primary reason is that the state-of-the-art localization algorithms[32, 52, 58] are dependant on the accurate location attributes of the WiFi access points (APs) in the physical maps of these airports and malls. To understand what we mean by location attributes, consider the setup shown in Figure 1(right). The smartphone user is triangulated in an indoor environment by estimating the angle subtended by the user at each of the access points. This approach inherently assumes to have accurate knowledge of each access point's location and its deployment orientation (the angle at which the access point is placed in the given physical map). Further, to estimate the angle made by the user with respect to an access point, the channel state information (CSI) based WiFi localization algorithms need to know the exact antenna placements on these access points.

One can endeavor to manually locate each of these access points in the environment, but they would be met with the following hurdles. First, these access points are usually not easily visible; they may be located behind a wall or pillar. Second, even if the AP is visible, most of the access points are encased by the manufacturer, making it difficult to know the exact information of the antenna placements on the access point. Third and finally, even if we can estimate the antenna placements on the access point from the datasheet provided by the manufacturer[1], the AP's *deployment orientation* has to be carefully calibrated to the indoor maps within an error of a few degrees.These obstacles make locating the access points a labor-intensive, time-consuming process and easily prone to human errors that are beyond tolerable ranges. Thus, we need a system that can help in accurate mapping of the existing WiFi infrastructure, which does not involve any manual labor or time.

In this paper, we present LocAP, an autonomous and accurate system to estimate access point location attributes – access point location, antenna placements, and deployment orientation. We call this process of predicting accurate access point attributes as *reverse localization*. LocAP is the first work to establish the requirements for reverse localization as follows:

Accurate Access Point Locations: As shown in Figure 2a,

[1]Datasheets may not always be publicly available, as in the case of Apple[6]

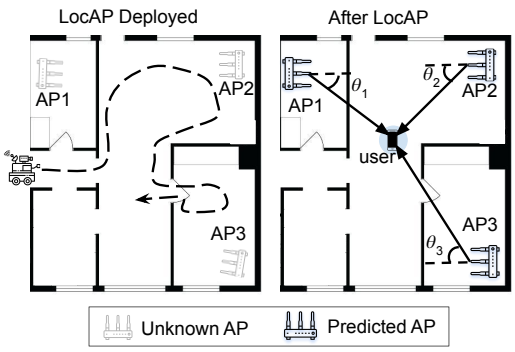

Figure 1: **Implementation of LocAP: (Left)** An unknown environment with unknown AP attributes. **(Right)** LocAP once deployed determines the AP attributes in the physical map enabling triangulation based user localization.

any error in AP location is translated to an error in the location of the user. So, any error exceeding a few tens of centimeters in access points' location is going to adversely affect the decimeter-level user localization. Thus, LocAP needs to locate the access point accurate to within a few centimeters. Unfortunately, existing indoor WiFi localization algorithms [32, 46, 52, 59] report localization accuracy up to tens of centimeters only, making it unfit for localizing access points.

Accurate Antenna Separation: Different APs have different antenna placement configurations and the angle made by the user is measured at the access point using the spacing between antennas. So, any error in measuring antenna placements is going to cause a rotation error at the user. For example, error in antenna separation by 4 mm causes 12^o of error in the angle of user measured at the access point, which translates to up to 1 m of error for a user 5 m away from the access point. Thus, LocAP needs to predict the antenna separation accurate to within a few millimeters.

Accurate Deployment Orientation: Finally, the access points can be placed in any orientation in the environment. Any error in measurement of orientation directly translates to the predicted angle subtended by the user at the access point. Hence even 10^o of error in deployment orientation causes up to 90 cm of user location error for a user located just 5 m away from the access point. Thus, LocAP should resolve the deployment orientation of the access point accurate to less than 10^o of error.

Automation: LocAP's goal is to require no manual effort for the reverse localization, and achieve the stringent requirements established earlier. Furthermore, there should be zero effort to connect these positions with existing indoor maps, ideally in an autonomous way.

LocAP achieves the aforementioned requirements and enables automated and accurate *reverse localization* of the access points. We achieve autonomy by deploying LocAP on a bot retrofitted with a multi-antenna WiFi device. When deployed in a new environment, the bot first maps the physical

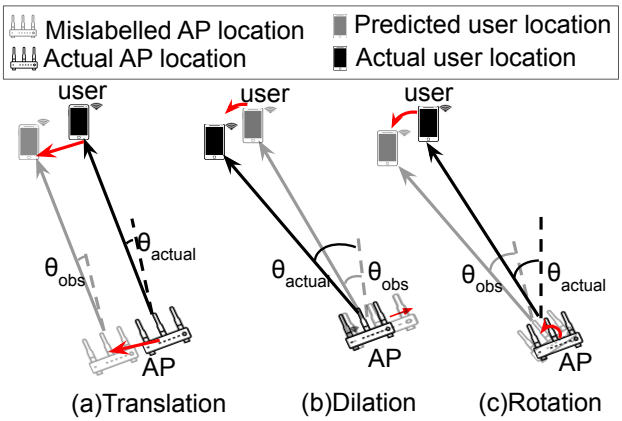

Figure 2: **Motivation for LocAP:** The user location is predicted wrong due to different errors in access point's estimated details. **(a) Translation:** Predicting the wrong location of the AP. **(b) Dilation:** Predicting wrong antenna separation on the access point results in an error in angle estimated,$(\theta_{obs} \neq \theta_{exp})$ of the user.**(c) Rotation:** Predicting the wrong orientation of the AP.

environment. Next, it associates with existing AP infrastructure by collecting multi-antenna channel state information, and pairing it with its predicted location in the physical map as shown in 1(left). LocAP uses this information to build a database of the deployed WiFi infrastructure consisting of all the access point attributes meeting our stringent accuracy requirements. This database can then be used for decimeter level user localization as depicted in Fig. 1(right)

The main technical contributions of LocAP to achieve the above requirements can be summarized as follows:

cm-accurate Access Point Localization: We make an important observation that accuracy of triangulation based WiFi-localization methods improves with an increasing number of anchor points with known locations. In essence, creating an array of 100's of antennas measuring CSI at known locations achieves cm-level localization, which is not feasible in practice[2]. To overcome this, LocAP leverages the CSI data collected by the bot at 100's of predicted locations, mimicking 100's of virtual antennas with known locations. However, these *predicted* locations suffer from a varying amount of inaccuracy. Hence, LocAP designs a weighted localization algorithm, which weights each location-CSI data-point with a uniquely defined confidence metric capturing the accuracy of the predicted location.

mm-accurate Antenna Geometry Localization: We have seen earlier that both mm-error in antenna separation and error in deployment orientation lead to in-accurate Angle of Arrival (AoA) measurement at the access point, which impedes user-triangulation. Thus, LocAP tackles antenna sep-

[2]typical indoor settings are 1000-2000 sq. ft., which would imply deploying an antenna every 100 sq. ft.

aration and deployment orientation together by achieving millimeter-level accuracy in predicting the antenna geometry. A first thought would be to use 1000's of virtual antennas to achieve cm-accurate localization [34] by locating individual antenna geometry on the AP. But, this idea will not suffice to achieve mm-level details of the antenna geometry. Our key observation is to localize the relative antenna geometry between two antennas, primarily because the relative channel between the two antennas can be measured very accurately by measuring the phase information. The phase information is measured at the carrier frequency level (λ=60 mm equivalent to 360^o), hence even phase measurement accurate to 10's of degrees achieves 1-2 mm accuracy. However, this works for only relative antenna separation $d < \frac{\lambda}{2}$. LocAP designs a novel algorithm which uses relative channel information across multiple bot locations to solve for any antenna geometry, unrestricted by antenna separation, to mm-level accuracy

Automation – Augmenting the SLAM algorithms: To avoid any manual labor and errors, we deploy Simultaneous Localization and Mapping (SLAM) based algorithms on the bot. The SLAM framework provides us with a physical map and the location and heading of the bot in this physical map at all times. We pair these location-heading measurements with the CSI collected by the mounted WiFi device. However, even the best of SLAM algorithms report the location to be in-accurate up to 10-20 cm, which can have a detrimental effect on the AP location attributes. Therefore, LocAP develops a confidence metric whose core idea to look at the quality of the relative transform between consecutive frames.

Further, the implementation of LocAP does not need any modification at the existing access points, as it is deployed using a Turtlebot[50] equipped with 4-antenna Quantenna [42] off-the-shelf reference design client. The Quantenna client readily reports the channel-state-information (CSI) of the associated access point. To evaluate LocAP, it is deployed in an indoor environment of 1000 sq ft area with multiple access points and 2 different antenna configurations – rectangular and linear[3]. For the access point, we localized commercial off-the-shelf Quantenna [42] QSR5GU-AX Plus, QSR10G and QSR2000C chipsets based access points and achieved the following results satisfying the aforementioned accuracy requirements:

Access Point Localization: LocAP's reverse localization of the access points achieves a median localization error of 13.5 cm improving by 35% over the state-of-the-art WiFi localization algorithms.

Relative Antenna Geometry Prediction: LocAP's relative reverse localization for the antenna separation has a median error of 3 mm (50× improvement), and a median error of 3^o(8× improvement) for deployment orientation, while state-of-the-art achieves a median error of 150 mm and 25^o respectively.

SLAM bot: Any error in bot' location and heading adversely effect LocAP's performance. So, we analyze the bot's localization error by making it follow a marked path and the median error reported was 16 cm. Our analysis shows that this error does not adversely affect LocAP's performance.

Case Study-User Localization: State-of-Art user localization is deployed using the access point attributes measured manually and with LocAP. We observe user localization errors of 70 cm and 50 cm respectively.

[3] these configurations generalize the more generic antenna deployments found on the commercial off the shelf WiFi access points.

2 Requirement and Motivation

It may seem natural that user localization algorithms[32, 46, 52, 59] could be sufficient for *reverse localizing* the access point's location attributes – location, antenna geometry and deployment orientation. Surprisingly, it turns out that requirements for reverse localization of the access are stringent. In order to define these requirements, we conduct empirical evaluations from the standpoint on how various errors in AP attributes adversely affect the state-of-the-art decimeter level localization algorithms.

Our empirical setup contains four access points, each with 4 antennas, setup in a 25ft×30ft space. The user device is placed at 100 different locations while the access points locate the user using an algorithm similar to [32]. Specifically, we aim to achieve decimeter-level localization accuracies for user WiFi localization algorithms and thus set a hardbound that no more than 50 cm median error for user localization can be tolerated.

Error in the AP's location Firstly, in the above-described setup, we incrementally increase the error in all the access points' locations. Next, we estimate the user location for each of these erroneous access point locations and calculate the user localization error. In Figure 3a, we plot the median user localization error across the access point errors reported. We can see that if the access point locations have an error of more than a few centimeters, the median localization error starts to increase. From this, we can infer that the required level of accuracy for the reverse localization of APs should be in the order of centimeters.

Error in the antenna separation Second, AoA based localization algorithms make use of the relative phase information between two antennas. Earlier, we have seen that the relative antenna position has to be estimated accurately to have exact measurements of angles. In fact, even when the access point positions are reported correctly, we can observe that the localization error increases with just a few millimeters of errors in the reported relative antenna positions as shown in Figure 3b. This observation is intuitive because the relative antenna distances are usually of the order of a wavelength of the transmitted signal, which in the case of WiFi is 6cm. So, any error which is greater than a few millimeters is going to make a huge difference in the relative phase measured at the access point.

Error in the Deployment Orientation Finally, the antenna

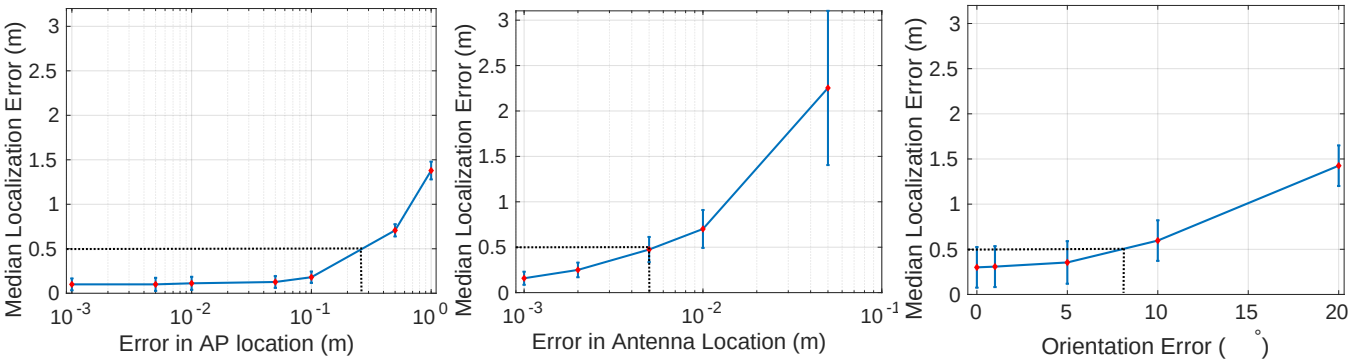

(a) (b) (c)

Figure 3: **Robustness of localization accuracy to Access Point (AP) location errors:**(a) Shows that median localization error increases with increase in error of estimated AP location.(b) Shows how median localization error increases with increase in error of estimated antenna locations. (c) Shows how median localization error increases with increase in error of estimated antenna deployment orientation.

array can be oriented in any direction. It is also important to know the exact deployment orientation of the antenna array. Errors in this orientation will proportionately affect the angle of arrival measurements made at the access points. In fact, we observe that the greater the error in deployment orientation prediction, the higher the median localization error becomes as shown in Figure 3c. From this plot, we can see that even 7^o will degrade the median user localization accuracy to more than decimeter level.

In summary, we should locate the access point's location with less than 30 cm of error, the antenna separation within 10 mm of error and the deployment orientation to less than 7^o of error. While these locations are typically mapped manually by humans using specialized equipment like VICON [48] or laser-based range finders[9], this process is time-consuming, labor-intensive and prone to errors. So, we need a system that can accurately localize access points attributes satisfying these stringent requirements. Note that the most stringent requirements are the mm-accurate antenna separation and sub-7 degree deployment orientation. The state-of-the-art [32, 34, 46, 59] localization algorithms can locate the individual antennas to within a few 10 centimeters even by deploying hundreds of AP's in a given environment, which is insufficient to determine the antenna geometry as per required specifications established earlier in this section. Further, there are tracking or relative localization algorithms[33, 53, 56] that can locate the user's location with respect to an earlier observation that is few millimeters apart. These tracking algorithms assume that the two relative locations are less than $\lambda/2$ apart but the antenna separations on most access points are more than $\lambda/2$ apart, where there is an ambiguity that cannot be resolved. So, we design a system, LocAP, which fulfills these requirements and locates the access points and their antennas with the desired level of accuracy

3 Design

In this section, we present LocAP's design. Recall that our main goal is to autonomously determine access points' location attributes accurately within the reference coordinate of the physical map to enable easily deploy-able WiFi-localization. LocAP deploys a SLAM based autonomous robot to map the environment. Then, LocAP uses this map to localize the robot using visual sensors to collect the locations and heading at each instance. Henceforth, we would define the pose of the bot as the combined location and heading measurements. Simultaneously, a WiFi device with 4 antennas is retro-fitted on the robot, which connects with the existing WiFi infrastructure, all the while collecting the CSI information at each instance. LocAP, therefore, is provided with the pose in the physical map and collects CSI data from existing WiFi infrastructure. We design LocAP to use these inputs to provide accurate access point attributes - location, antenna separation, and deployment orientation.

First, we discuss how to achieve the cm-level accurate location of the AP despite the inaccuracies in reported robot poses. Second, we present LocAP's algorithm to learn the antenna separation and deployment orientation of the AP's as it is the most challenging, and needs to achieve the stringent requirement of mm-level accuracy. In both of these scenarios we assume we have the CSI corresponding to the direct path and thus in Section 3.3 we discuss how we tackle the problem of multipath in both of these scenarios. Finally, we present the SLAM-based bot design, which does the best effort to provide the necessary measurements mentioned above. But often, these measured poses are not accurate. So, LocAP builds an algorithm which reports a confidence metric for each measured pose. This confidence metric helps us surmount the errors in the bot locations to calculate AP location attributes.

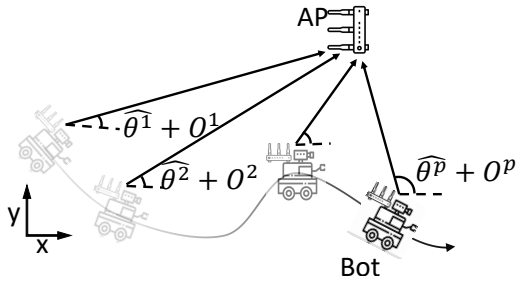

Figure 4: **First Antenna Localization:** Gives an overview of how triangulation from 10s of bot locations locates the access point accurately to within few centimeters.

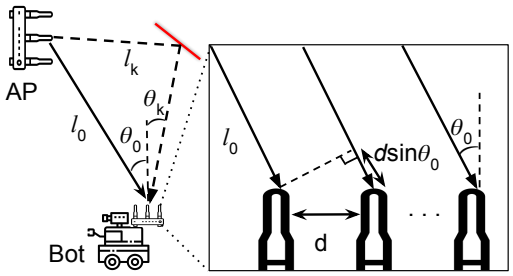

Figure 5: **CSI based angle-of-arrival(AoA) measurement:** For each of the multiple reflections, the additional distance travelled by the incident signal on the 2^{nd} antenna with respect to the 1^{st} antenna can be measured as $d\sin\theta_k$ under the far-field assumption.

3.1 Locating the Access Point

First, we discuss how we can identify the location of the access point. Specifically, in this subsection, we focus on identifying the position of one of the access point antennas. This position of the antenna would then be representative of the access point's location. We call this antenna as the first antenna in the subsequent text. Recall that the access point's location has to be estimated accurately to cm-level. A simple solution can be to utilize the existing WiFi localization approaches to locate one of the antennas on the access point, which would then become the access point's location. However, state-of-the-art localization algorithms only report decimeter level location estimates. We make an interesting observation: these algorithms show increasing location accuracies with an increase in the number of access points deployed in an environment. Unfortunately, a typical indoor environment only has 4-5 access points, while achieving cm-accurate location estimates requires at least a few 10s of access points. However, LocAP is deployed on an autonomous bot equipped with a WiFi device enabling it to collect both CSI and also the location and heading of the bot and thus of the WiFi device atop. This setup enables us to collect location labeled CSI across tens of known bot locations, creating 10s of virtual anchors.

Owing to this setup of LocAP,we can employ AoA estimation algorithm similar to [32] to estimate the direct path's angle of arrival, $\hat{\theta}^p$, corresponding to the first antenna's transmission for each bot location $\mathbf{u}_p = [u_p, v_p]$. To enable this AoA based first antenna triangulation we should also know the direction of the bot's heading (O_p), which is reported by the bot as mentioned earlier. With ($\mathbf{u}_p, O_p$ and $\hat{\theta}^p$) we can find the first antenna location as an intersection of P lines defined as:

$$Line_p \equiv (y - v_p) = \tan(\hat{\theta}^p + O^p)(x - u_p) \tag{1}$$

Ironically, the AoA based triangulation for a single antenna depends on the errors in the bot's reports of its location,(u_p, v_p) and heading, O_p. This creates an infinite loop where to locate the access point accurately we need to know the bot's location accurately and to know the bot's location accurately we need to know the access point's location accurately. To overcome this problem, we take advantage of bot's SLAM algorithm. SLAM based bots do not have 100% confidence in the location estimates they report. Based on this intuition, we design a confidence metric, $w_p \in [0,1]$ for each bot location $\mathbf{u}_p$. Further details on the design of the confidence metric are discussed in Section 3.4. This confidence metric implies that the bot is more confident with the reported pose the closer it is to one. We thus first implement a smart low-confidence rejection algorithm, where we neglect the last 20% of the datapoints when sorted in the descending order of their confidence levels. We then use the confidence metric in combination with the rest of our $0.8P$ line equations to define a weighted least squares problem to optimally solve for the first antenna location as follows:

$$\min_x ||W(S\mathbf{x_1} - \mathbf{t})||^2 \tag{2}$$

where $W = \text{diag}(w_1, w_2, \cdots, w_0.8P)$ is the weight matrix, $S(p,:) = [\sin(\hat{\theta}^p + O^p) \quad -\cos(\hat{\theta}^p + O^p)]^T$ and $\mathbf{t}(p) = [u_p \sin(\hat{\theta}^p + O^p) - v_p \cos(\hat{\theta}^p + O^p)]$.

3.2 Determining Antenna Separation and Deployment orientation

As described above, we can leverage the motion of the bot to identify the accurate location of one antenna on the access point. One might wonder if it is possible to apply this algorithm iteratively to identify the location of each antenna on the access point and hence recover the relative placement of antennas. However, it is not so straightforward. In particular, the geometry prediction needs to be an order of magnitude more accurate than the location prediction. While it suffices to measure the location of the access point to cm-level, the geometry, i.e. the relative position of antennas, needs to be mm-accurate. While combining across 10s of bot locations provides antenna location accurate to cm-level, it does not extend to mm-accurate antenna geometry by combining across 100s or even 1000s of bot locations as shown in the prior art[34]. This

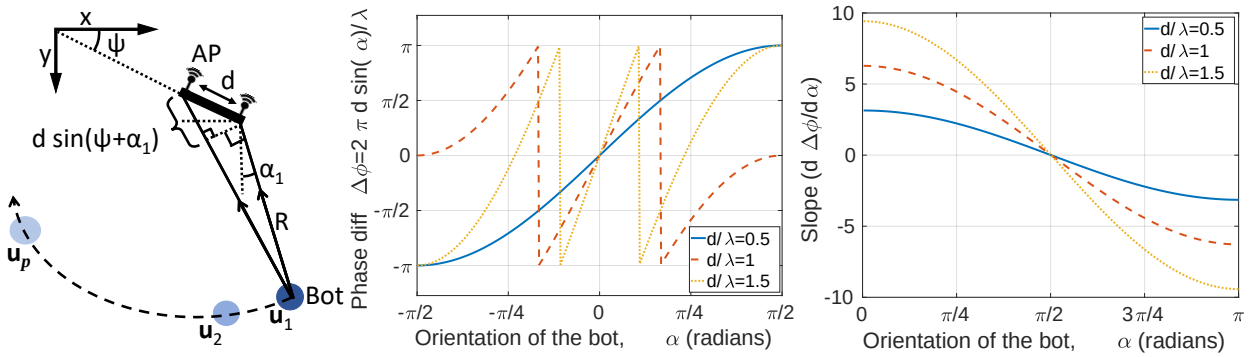

(a) (b) (c)

Figure 6: **Estimating AoD from phase difference:** (a) A sample case where the bot is in circular arc around the AP (b) Phase difference $\Delta\phi$ vs the orientation of the robotα when compensated for the orientation of the access point (c) Slope $\frac{d\Delta\phi}{d\alpha}$ vs the orientation of the robotα when compensated for the orientation of the access point.

problem occurs owing to the asynchronous clocks between the access point and the bot's WiFi device when measured at a single antenna at the access point.

To overcome this problem we make a key observation - in contrast to the phase measured at one antenna on the access point, the relative phase across two antennas is rid of synchronization errors as they share the same clock. Further, for the 5GHz carrier frequency WiFi 11ac usually operates on, the wavelength is 6 cm, which corresponds to a phase difference of 2π radians. Usually, we can easily resolve phase differences up to $\pi/18$ radians (10^o), which facilitates measurement of the distance between two antennas with a resolution of 2 mm, thus enabling us to locate the antenna geometry accurately to within few millimeters. Hence, our first key insight is to measure the relative antenna separations, d_i, and deployment orientations, ψ_i, of all the antennas on the access point with respect to the first antenna. ($i = 2, 3, \cdots, N_{ap}$)

Unfortunately, although the relative phase information is able to resolve relative antenna separation to within 2mm, it cannot resolve for antenna separations greater than $\lambda/2$. To further understand this, consider an example scenario where the bot is moving in a circular arc about the two antenna access point in steps of small angles as shown in Figure 6a. Now to locate the second antenna with respect to the first we know that for the bot's location, $\mathbf{u}_p$ along the arc, the phase difference corresponding to the direct path, $\Delta\phi_p$, can be estimated as:

$$\Delta\phi_p = \mod\left(\frac{2\pi d}{\lambda}\sin(\psi+\alpha_p), 2\pi\right) \tag{3}$$

where, ψ and d are antenna deployment orientation and antenna separation respectively, the parameters of interest, for the given scenario. α_p is the angle made by the bot's location at the access point with respect to the global Y-axis. We plot this $\Delta\phi_p$ for all the bot locations along the circular arc against bot's orientation, α_p for various d in Figure 6b. From this plot we can see that though for $d \leq \lambda/2$ we have a unique mapping between the phase difference, $\Delta\phi_p$ and the bot's location, for $d > \lambda/2$ we have ambiguous solutions. The ambiguity occurs because the phase difference we measured is a mod of 2π, which means for a given $\Delta\phi_p$, the actual phase difference can be $2n_p\pi + \Delta\phi_p$, where n is any positive integer. This means we have three unknowns, (d, ψ, n_p) to solve for, given a single phase difference value, $\Delta\phi_p$. Furthermore, for each additional bot location we have a new $\Delta\phi_{p+1}$ estimate, and we also add an extra unknown n_{p+1} making it impossible to uniquely solve for d and ψ. In contrast to the phase difference $\Delta\phi_p$, the differential phase difference with respect to the bot's angle at the AP (α_p) for optimally small increments of α_p, has a unique one-to-one mapping as shown in Figure 6c. So, the second key observation we make is that while the phase difference is not uniquely solvable for $d > \lambda/2$, the differential phase difference is uniquely solvable.

In fact, LocAP does not restrict the bot's motion to a circular arc and can work with arbitrary motion, as long as the CSI is measured regularly. To understand the exact implementation of LocAP's relative antenna geometry prediction we consider a more free-flow path as shown in Figure 7. To avoid over-crowding of subscripts, we consider just one more antenna and drop the antenna indexing, i. Similar analysis can be performed pairwise on all the antennas on the access point with respect to the first antenna. To solve for the relative geometry between a pair of antennas, we have to solve for both the distance between antennas, d, and the deployment orientation of the antenna array, ψ, as can be seen from Figure 7. The bot moves to P different locations about the AP and collects a series of P CSI measurements, H_p ($p = 1, 2, \cdots, P$), while simultaneously reporting its locations, $\mathbf{u}_p$. Note that we use a single antenna at the user's WiFi device. The WiFi device makes an angle α_p from the positive y-axis in the global coordinate system at the p^{th} position for $p = 1, \cdots, P$. For each position of the bot, $\mathbf{u}_p$, we measure the differential phase difference $\frac{d\Delta\phi_p}{d\alpha_p}$ between the two antennas on the access point

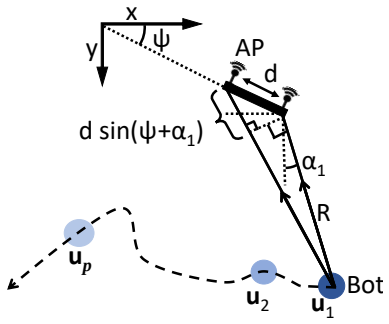

Figure 7: **Relative Geometry Prediction:** Shows a simple two antenna AP making angle ψ with the positive x-axis and the robot moving about the located first antenna of the AP making an angle α_p at it's p^{th} location. For this setup the extra distance travelled by the signal to the second antenna is $d\sin(\psi+\alpha_p)$.

using the CSI measurements made at that position as

$$\frac{d\Delta\phi_p}{d\alpha_p} = \frac{2\pi d}{\lambda}\cos(\psi+\alpha_p) \tag{4}$$

where we can see that $\theta_p = \psi+\alpha_p$ is the angle of arrival (AoA) at the AP from the WiFi device for the position p. Although α_p can be determined from the location of the bot, θ_p is not known as ψ is a parameter to be determined. For incremental movements of the bot, the differential phase difference in Equation4 can be approximated as

$$\frac{d\Delta\phi_p}{d\alpha_p} \approx \frac{\Delta\phi_{p+1}-\Delta\phi_p}{\alpha_{p+1}-\alpha_p} \tag{5}$$

Note that the above approximation works well when the robot moves along a direction perpendicular to the Line-of-Sight(LOS) path. However, we do not just have two or three locations of the robot, the robot traces $P(>3)$ positions as it moves. This enables us to obtain the solution from an over-determined system of equations, consequently reducing the noise level, achieving highly accurate relative antenna position and orientation, and thereby achieving millimeter-level accuracy for relative antenna localization. Now to solve for (d,ψ) uniquely as an over-determined system, it is easier to work with Cartesian co-ordinates than polar coordinates. So, we fix the location of the first antenna of the AP and represent the second antenna coordinates (x,y) defined by the global coordinate system as $(x,y) = (x_1 - d\cos(\psi), y_1 - d\sin(\psi))$, where $\mathbf{x}_1 = [x_1\ y_1]^T$ is the first antenna's location. We can then rewrite equation (4) in terms of (x,y) as follows:

$$\frac{d\Delta\phi_p}{d\alpha} = \frac{2\pi}{\lambda}((x_1+x)\cos(\alpha_p) - (y+y_1)\sin(\alpha_p)) \tag{6}$$
$$\text{for} \quad p = 1,2,\cdots,P-1$$

We can rewrite these P set of linear equations in vector form as follows

$$A\begin{bmatrix}x+x_1\\ y+y_1\end{bmatrix} = \mathbf{b} \tag{7}$$

where A is a $(P-1)\times 2$ matrix and b is a $(P-1)$ sized column vector defined as

$$\begin{aligned} A(p,:) &= \begin{bmatrix}\cos(\alpha_p) & -\sin(\alpha_p)\end{bmatrix} \\ \mathbf{b}(p) &= \frac{\lambda}{2\pi}\frac{\Delta\phi_{p+1}-\Delta\phi_p}{\alpha_{p+1}-\alpha_p}, \quad p = 1,2,\cdots,P-1 \end{aligned} \tag{8}$$

We can further denote $\mathbf{x} = \begin{bmatrix}x & y\end{bmatrix}^T$ to solve for the following least squares problem:

$$\min_{\mathbf{x}} \quad ||A(\mathbf{x}+\mathbf{x}_1)-\mathbf{b}||^2 \tag{9}$$

Thus we can uniquely solve for the cartesian coordinates of the second antenna with respect to the first antenna.

Note that the two measurements $\{\alpha_p, \Delta\phi_p\}$ and $\{\alpha_{p+1}, \Delta\phi_{p+1}\}$ should not be very close to avoid noise amplification. On the other hand, the measurements should not be very far away to cause an error in the estimation of the derivative where the phase change across these two locations become more than 2π thus making the phase difference discontinuous across various angles. Our experiments suggest that around 10^o of angular separation $\alpha_{p+1}-\alpha_p$ provides the best results for an antenna separation, $d = [0, 2\lambda]$, where $\lambda = 6$cm is the minimum wavelength in the 5GHz frequency band. Any higher range of antenna separation would need much finer angular separation. Our experiments suggest that 5° provides the best results for $d \leq 4\lambda$. We emphasize the estimated value of ψ will be in the range of $0 \leq \psi \leq \pi$ because the orientation of the antenna array can be defined uniquely in $0 \leq \psi \leq \pi$.

Using Equation 9, we can locate the relative location of each antenna on the access point as $\mathbf{x_i} = [x_i \quad y_i]^T$, where, $i = 2,3,\ldots,N_{ap}$, where N_{ap} are the number of antennas on the AP. Hence, we can find the antenna separations, d_i and the deployment orientation, ψ_i for all the antennas with respect to the first antenna,$\mathbf{x}_1$. Thus accurately predicting the location, antenna separation and deployment orientation of the access point.

3.3 Multipath

So far, in both Section 3.1 and Section 3.2 we have assumed only one single path from the AP to the bot to solve for the access point attributes. However, the environment creates multi-path which would cause the previous algorithms to fail by distorting the phase measurements considered in Section 3.1 and Section 3.2.

Specifically, in Section 3.1 we assume one singular direction to the AP from the bot which may not always be the case. However, in this scenario, the multiple antennas on the bot

along with the bandwidth of the WiFi signal would help us to identify the direct path and separate it similar to prior art[32]. Thus we implement an algorithm similar to[32] to estimate the angle of arrival corresponding to the direct path from the bot to the AP. Thus we solve for the multipath issue for the first antenna or access point localization.

Further, in Section 3.2 we assume that we know the exact phase difference across two antennas corresponding to the direct path which is not so straightforward. As unlike in Section 3.1 we cannot directly measure the angle at the access point since both the antenna separation and deployment orientation of the AP are not known, which are key parameters to estimate the angle of arrival. So we exploit the multi-antenna setup on the LocAP's autonomous bot to resolve the multipath where we make a key observation, that channel is usually reciprocal. That is the direct path from the AP to the bot is the same as the direct path measured from bot to the AP. However, to identify the direct path's phase using the MUSIC algorithm is not accurate as MUSIC results in a weighted output. So we employ a 2D FFT based projection from the frequency-antenna space to AoA-ToF space as described in [7]. In this setup, we can identify the direct path and the exact peak's representation in a given neighborhood and extract the direct path as the least ToF peak, which is similar to [32]. We can do this because we know the antenna separation on the WiFi AP and the exact location and heading of the bot at all times. Thus we identify the AoA-ToF neighborhood corresponding to the direct path from the bot to each individual antenna on the access point to be located and then perform and 2D-IFFT to get the direct path's phase for each antenna on the access point.

Furthermore, if we have CSI with high multi-path making the direct path identification impractical we can choose to drop the measurement as we have a larger number of data points.

3.4 LocAP's Bot Design

In the following section, let us look more closely at the autonomous bot. We deploy the bot largely to automate our data collection pipeline. The key pieces of data we need to collect are the robot's pose information, (u, v) locations and orientation α, time-synchronized CSI estimates for each AP in the environment and the confidences for our pose measurements. Most widely available SLAM algorithms provide time-stamped pose information. This bot is retrofitted with an RGBD camera, hence we also acquire the color and depth frames for each pose measurement, allowing us to generate point-clouds. Furthermore, a key feature of LocAP is it's robustness to the path followed by the robot. As mentioned earlier, as long as the bot moves slowly (less than 15 cm/s), maintaining a comfortable distance with the AP's (more than 5-10 m), we will get accurate results with LocAP. An important point to note is that collecting a pose and CSI measurements from a diverse range of AoA's at the AP's end will increase LocAP's accuracy.

Now, let us understand the confidence metric we mentioned earlier. Unfortunately, most SLAM algorithms do not expose the confidences of a particular pose estimate. Hence, we make the following observation - by looking at the registration accuracy of the point-clouds generated by consecutive pose measurements, we can estimate the quality of the relative transformation in question. More concretely, let's consider two consecutive frames $\mathcal{F}_i$ and $\mathcal{F}_{i+1}$. We can determine the relative transformation T_i between the two frames by looking at their pose estimates. Hence, T_i takes us from $\mathcal{F}_i$ to $\mathcal{F}_{i+1}$. Furthermore, from the RGBD images captured at these frames, we can generate point-clouds. By applying the T_i to the point-cloud from $\mathcal{F}_i$, we can stitch these two point-clouds together. If T_i is accurate, then we will get a perfect stitch. Based on this intuition, we use the covariance matrix $\mathcal{V}_i'$ as implemented by [14]. Now, this covariance matrix accommodates all six degrees of freedom as found in a 3D environment, hence $\mathcal{V}_i' \in \mathbb{R}^{6\times6}$. The first two diagonal elements give us the variance in the x and y position and $\mathcal{V}_i'[1,2]$ gives us the co-variance between x and y. The variance in $(x+y)$ tells us how much wiggle room there is for the pose in question. Hence, the larger the wiggle room, the less confident we are in our poses. Furthermore, we observe that these variances vary in orders of magnitude, and to linearize our confidence metric, we take the log of the variance. We calculate the confidence metric for $\mathcal{F}_i$ as

$$C_i = \log(\text{var}(x+y)) \tag{10}$$
$$= \log(\text{var}(x) + \text{var}(y) - 2\text{cov}(x,y)) \tag{11}$$

Finally, we normalize C_i, $\forall i = 1, 2, \cdots, P$, to determine w_i.

4 Implementation

In this section, we describe the hardware implementation in RevBot. The key design criterion for LocAP was to come up with a system that is capable of accurately reverse localizing the access points and their antenna geometries while eliminating significant manual effort. Thus, we deploy RevBot, a ROS-based robot employing SLAM algorithms to provide accurate pose measurements. This robot is able to traverse the unknown environment and report the ground truth values for its current location by running RTAB-Map [35]. Furthermore, it is retrofitted with a WiFi device, provided by Quantenna [42], serving two purposes. First, it provides us with the opportunity to automate the reverse localization system; and second, it allows us to associate CSI estimates with ground truth labels. Concretely, the WiFi device mounted on the robot is used to communicate with the APs in the environment and collect CSI on the received messages. These CSI estimates are given context by the ground truth estimates obtained from the robot. It is important to note that although we state that the

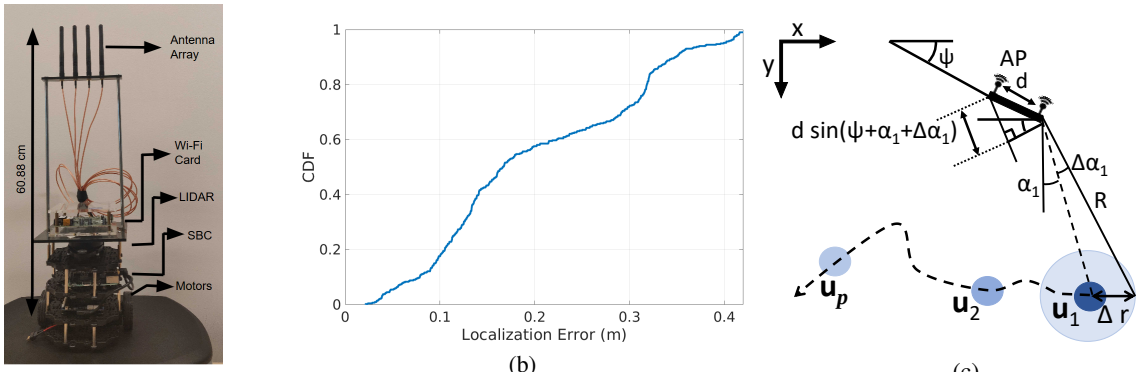

(a) (b) (c)

Figure 8: **Accuracy of the bot's ground truth movement:** (a) The bot we used for our experiments.(b) The median ground truth error for the bot's ground truth. (c) An example depiction on how Figure 7 is affected by the bot's error and thus the relative antenna localization.

CSI estimates and pose information are time-synchronized, the WiFi device and the robot have independent clocks. To match the pose information with the corresponding CSI estimate at that location, we begin by collecting a sync packet. Next, the time of the first received packet is matched to the time of the first pose reported by RTAB-Map. We use these times as the start-times for both the WiFi device and the pose measurements. These paired CSI estimates and pose information are passed to LocAP.

5 Micro-benchmarks

Before evaluating LocAP's performance, it is important that we understand how the error in the ground truth locations reported by the autonomous bot is effecting the algorithm. For that, we first estimate the bot's location error and analyze its effects on the accurate prediction of the location of the access point and the relative antenna geometry on the access point.

5.1 Error in Bot's ground truth Location

We estimated the ground truth error by first traversing a circle (radius = 2.8 m) three times, for a total path length of about 50 m. Next, we find the best-fit circle to our path and use this as the ground truth. The CDF plot for error between RTAB-Map's reported error and the best-fit circle is shown in Figure 8c. We can observe that the median error is around 16cm in this case. Further, we study the orientation errors within the same setup. We use the tangent to this best-fit circle as ground truth orientation. We find that the median error in orientation is 3°

Next, we analyze the effect of this error on the accuracy of locating the access point and determining the relative antenna geometry.

5.2 Effects of Bot's Error

First, we estimate the location of the access point. For this step, we use both the bot's location and orientation. Hence, we must look at the errors in both these measurements. We observe that an error of Δr in bot's location error directly corresponds to an error of Δr in the access point's location prediction. Next, assuming an orientation error of ΔO, we observe that the error will be $R\Delta O$ in the access point's location, where R is the estimate of the distance to the access point. Hence, the upper-bound on the total error propagated will be $\Delta r + R\Delta O$

Second, for the relative antenna location estimation, from Figure 8b we can see that the error in bot's location, Δr, translates to error in the angle estimated at the access point, $\alpha_i + \Delta\alpha_i$, where we can write $\Delta\alpha_i = \frac{\Delta r}{R}$. Hence, we get $A' = A \begin{bmatrix} 1 & \frac{\Delta r}{R} \\ -\frac{\Delta r}{R} & 1 \end{bmatrix}$, while b remains unchanged. Thus we can re-write Equation 9 as

$$\min_{\mathbf{x}'} ||A'\mathbf{x}' - \mathbf{b}||^2 \tag{12}$$

where $\mathbf{x}' = \mathbf{x} + \Delta\mathbf{x}$, and $\Delta\mathbf{x} = \begin{bmatrix} \Delta x & \Delta y \end{bmatrix}^T$. Solving for $\Delta\mathbf{x}$ from the Equations 9 and 12, and simplifying by neglecting higher order error polynomial terms we can see that $\Delta x = \frac{\Delta r}{R} y, \quad \Delta y = \frac{\Delta r}{R} x$. We know that $\mathbf{x} = [x \quad y]^T$ is of the order of few centimeters, while Δr is of the order of few centimeters and R of the order of few meters, which reduces the whole expression for Δx and Δy to be of order of $\frac{1}{10}^{th}$ millimeter, which is well within limits of the tolerance for relative antenna localization. Thus we observe that the relative antenna geometry on the access points can be estimated accurately to within few millimeters using LocAP and its implementation on our autonomous system.

6 Evaluation

This section details the tests carried out to evaluate the performance of LocAP to see if it has delivered on its goals pre-

sented in Section 2. For this, the autonomous bot of LocAP was tested extensively in two different indoor environments spanning an area of around 1000 square feet. Multiple access points were deployed across these two environments at different locations, heights, and orientations. We have also deployed access points with linear and square antenna arrays. Over these multiple deployments, we have covered 8 different access point locations with 5 different antenna separations, $\{\lambda/2, \lambda, 3\lambda/2, 2\lambda, 5\lambda/2\}$, where $\lambda = 2.6$cm is the minimum wavelength in the 155 channel of the 5GHz frequency band. Over the course of this experiment, we collect CSI from multiple access points across space and time which is used to implement LocAP. The ground truth for all the evaluations are measured accurately with a commodity laser range finder[9], that is accurate to up to 1mm, after carefully marking the axes on the ground and labeling the 1000 sq ft space of experimentation. This entire process of labeling the experimental space of 1000 sq ft takes a minimum of one hour spent by a group of at least two people. While there is two decades of CSI based WiFi localization, LocAP is the first work to tackle the problem of *reverse localization* of the WiFi access points and thus is compared with a state-of-the-art AoA based user localization algorithms[32, 59] which combines data across multiple bot locations.

With the given setup the overview of LocAP's results are as follows: LocAP achieves 13.5cm of median localization error for the first antenna localization utilizing the weighted least squares formulation while a simple least-squares problem achieves just 20.5cm of median localization error. Further, the relative geometry prediction algorithm of LocAP locates the access points in this setup accurately with a median antenna separation error of 3 mm and a median orientation error of 3^o, whereas the state-of-the-art localization algorithms achieve a 1.5 cm median error for antenna separation and 25^o median deployment orientation error.

A final case study of user localization with the updated LocAP's AP attributes showed a reduction of 20 cm in median user localization compared to the manual AP attribute mapping.

6.1 AP Location accuracy

To evaluate the access point localization accuracy of LocAP, we deploy the system in 8 different test scenarios across various heights of access points, different location, environments and distances from the bot. To get a statistically accurate estimate of these locations, we have collected the CSI corresponding to each of these locations at 20 different time instants. With this data, we have estimated the location of each individual antenna on these access points as described in LocAP's design, Section 3.1. We also implement a least-square triangulation algorithm[32, 59] as a comparative baseline model, and we observed that while the baseline model provides a median AP localization error of 20.5 cm our weighted

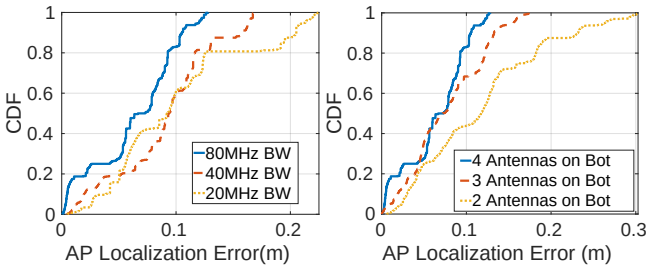

(a) (b)

Figure 9: **Single Antenna Localization accuracy:** (a) Shows how the localization error of locating a single antenna on each AP varies for various Bandwidths. (b) Shows how the localization error of locating a single antenna on each AP varies for various number of antennas on the Client on the autonomous bot.

least squares with smart-rejection achieves 13.5 cm showing an improvement of 36% in AP localization.

Further, the bandwidth assumed for these initial results is 80MHz, while the commodity WiFi access points hardly operate at these bandwidths. These WiFi access points usually use either 20MHz or 40MHz bandwidths. To mimic this, we also collect CSI data with the same setup for both 40MHz and 20MHz bandwidths. These CSI estimates have then been utilized to test our algorithm at different WiFi bandwidths. The CDF plot for variation of localization accuracy across different bandwidths can be seen in Figure 9b. It is clearly seen that at higher bandwidths, the localization accuracy is marginally better, while LocAP still attains centimeter-level accuracy for localizing the access point.

The design of LocAP relies on the angles estimated from the CSI data received. While the above-reported results are for a 4-antenna station, a commodity off-the-shelf WiFi device does not always have 4 antennas. Hence, we performed another experiment to observe the effect of change in the number of antennas on LocAP. This was done by changing the number of antennas present on the station mounted on the mobile robot. The CDF plot for the localization error with the increasing number of antennas can be seen in Figure 9c. The localization accuracy increases with the increasing number of antennas on the client mounted on the mobile robot. This is evidenced by the lower median error observed with 4 antennas present on the mobile robot as seen in Figure 9c. We further observe that a 2 antenna WiFi device significantly hurts the performance of LocAP as this would give an angular resolution of about 90° in space making it hard for the robot to resolve the exact direction of the access point.

6.2 Relative Antenna Geometry Accuracy

After the location of the first antenna of the AP is obtained, LocAP finds the positions of the other antennas of the AP relative to the first antenna. This is achieved by traversing

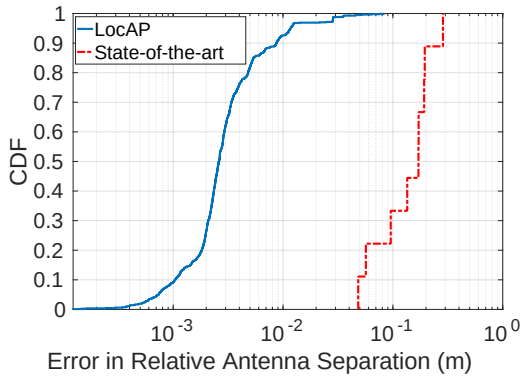

Figure 10: **Antenna Separation:** CDF plot of error in measuring antenna separation across 8 different Access point deployments

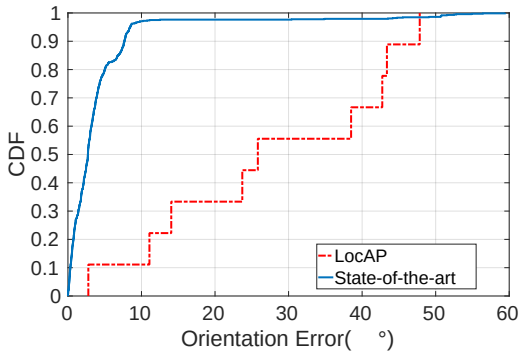

Figure 11: **Deployment Orientation:** CDF plot of error in measuring deployment orientation across 8 different Access point deployments

around the reverse localized antenna of the AP, as described in Section 3.2. To test this algorithm, we deploy APs with a linear antenna array and a square antenna array AP in the two aforementioned environments. Similar to AP location estimation, we have collected data for each antenna setup at 40 different time instances to obtain statistically accurate results. The relative antenna locations on these APs were measured using LocAP and then compared with the ground truth to get the relative antenna localization errors and the deployment orientations.

Relative Antenna Separation: We first measure the relative antenna separation of all the antennas on the access point with respect to the first antenna and the CDF plot for the errors in relative antenna localization is shown in Figure 10. We can see that the median error is about 3 mm for the relative antenna localization of LocAP while the state-of-the-art WiFi localization algorithm combined over multiple bot locations and time instances achieves 20 cm of median antenna separation error. Thus we show that LocAP achieves millimeter-level accuracy, (< 10 mm limit set in Section 2) for predicting the antenna separation of the access point.

Deployment Orientation: We also measure the deployment orientation of all the antennas on the access point with respect to the first antenna and the CDF plot for the errors in the deployment orientation is shown in Figure 11. We can see that while the state-of-the-art localization algorithm has a median error of 25^o, LocAP's deployment orientation prediction algorithm achieves a median orientation error of just 3^o ($< 7^o$ limit set in Section 2)

6.3 Case Study:User Localization

So far we have seen the performance of LocAP in accurately predicting the access point attributes. We implement LocAP, to enable CSI based indoor user localization. Further LocAP is automated by deploying on a bot to remove any manual labor or human errors. We thus verify the effect of both LocAP mapped AP attributes and manually mapped AP attributes on the state-of-the-art indoor WiFi localization algorithms[32, 46, 59]. To this end we have asked a group of ten people to measure the locations of four access points, their antenna separations and deployment orientation in a 1000sq ft space where LocAP has been deployed using a laser range finder[9] and a vernier calipers. From these user measurements, we have observed that manual mapping can make their best efforts to map the AP locations accurate with 15 cm median error and the antenna separation accurate to within 5 mm of median error. But these people fail to identify errors in deployment orientation and thus had an error greater than 10^o measured in deployment orientation measurements.

We then deploy LocAP in the same 1000 sq ft environment and locate the same 4 access points' attributes. A moving user that covers 300 different marked locations in this environment is then localized using both the manually mapped and LocAP's mapped AP attributes and the corresponding CDF is shown in Figure 12. From this plot, we can see that while human mapped AP attributes have a median localization error of 70 cm, LocAP's AP locations achieve 50 cm median error. Thus we can see that LocAP solves for the fundamental dependency of CSI based user localization algorithms by accurately predicting the AP attributes within the physical map.

7 Related Work

There has been significant work in the field of localization and LocAP's implementation work on reverse localizing the access points is closely related to the work in the following three fields:

Indoor Localization: Wide-scale deployment of WiFi based infrastructure and WiFi chips on hand-held devices makes indoor localization promising for various indoor navigation applications. There has been extensive research in WiFi based indoor localization algorithms over the past two decades [8, 13, 18, 19, 25, 32, 34, 36, 38, 40, 45, 46, 51, 52, 57–61, 64, 66]. While most of the initial work was based on the Received

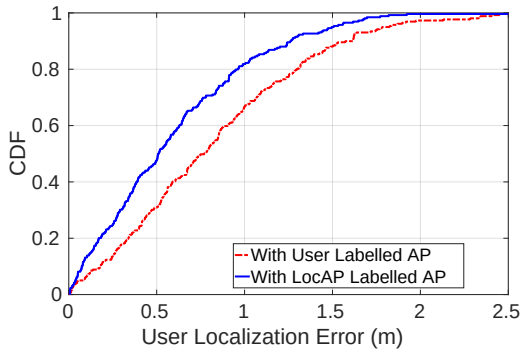

Figure 12: **User Localization accuracy:** Shows the CDF of localization accuracy after localizing the access points with LocAP and compared with those results of the manually labeled APs.

Signal Strength Information [8, 13, 40, 66] these algorithms do not achieve meter-level localization, or require extensive fingerprinting to achieve desired decimeter-level localization. Thus, most of the later work has been focused on CSI based localization algorithms [18, 25, 32, 34, 45, 46, 51, 52, 57–61]. LocAP which leverage the idea of Angle of Arrival based localization. Some such algorithms which have been developed in the past few years [32, 59] achieve decimeter-level localization and extend it to achieve centimeter-level localization accuracy. However, these WiFi based localization algorithms assume the knowledge of the location of the AP to measure the user's location with respect to the AP location. In contrast to the above work, LocAP builds a relative localization technique which provides millimeter-level accuracy for the antenna geometry on the AP. Furthermore, we also demonstrate that LocAP can solve for the antenna separation values larger than a single wavelength (λ).

Source Localization: Solving the problem of accurate knowledge of the WiFi AP locations have been attempted for RSSI based [22] and CSI based [47] systems. But these algorithms do not achieve centimeter-level localization for APs, but solve for the general regional mapping of these access points. These works are limited by the available bandwidth and thus there has also been significant work on ultra-wideband (UWB) based localization [5, 11, 12, 15, 29, 41, 43] and anchor localization algorithms [10, 16, 17, 29–31]. But these UWB systems require new infrastructure deployment. Similarly, there has been significant work towards a beacon based localization system [7, 24, 27, 28, 37, 54, 55, 62, 63, 65] which have been shown to achieve decimeter-level localization but also need additional deployment of infrastructure. LocAP solves the problems of exact WiFi access point localization and exact antenna placements on WiFi Access Points.

Relative Localization: LocAP solves for millimeter-level accurate antenna placements on any given WiFi access point by borrowing and extending the principles from wireless tracking. Wireless tracking or relative localization is a well-solved problem unlike localization, with reported accuracies up to few centimeters and few millimeters [33, 53, 56]. Though all of these algorithms would need the separation between two consecutive locations to be tracked to be less than $\lambda/2$ distance apart, LocAP solves for relative localization of two antennas that are at any arbitrary distance from each other, including for distances greater than $\lambda/2$ apart. Thus LocAP can enable high mobility tracking for indoor WiFi devices.

SLAM Automation: There has been exhaustive research conducted in graph based SLAM algorithms[20]. In LocAP we employ a SLAM based autonomous bot to report ground truth and also design a metric to understand the confidence of the bot for a given ground truth. Confidences for reported measurements can be extracted from the marginal co-variances of the nodes used to describe these variables and are used to perform data association [23, 26, 39, 49]. Though these numerical methods are valid, most of them are not implemented on standard SLAM platforms, to the best of our knowledge. Furthermore, commonly used frameworks[21, 35] do not readily expose these marginal co-variances. We extend the methods described in [14] as a proxy for these internal co-variance metrics.

8 Conclusion

We presented automated reverse localization of WiFi APs was successfully achieved as validated by the aforementioned results. Initial results obtained in our testing environment provided an accuracy of 10cm and lesser for the reverse localization of the access point, and an error of under 10 degrees for the orientation of the access point. As mentioned previously, using the mapping and reverse localization information, we can provide accurate indoor localization and navigation for large indoor environments.

After the mobile robot is allowed to traverse the unknown environment, we have a map of the indoor environment and the reverse localized positions of all the APs in this environment. If we consider the map to be part of a coordinate system, we can provide each access point with its own coordinate in the environment, such that the AP becomes self-aware about its location. When a new user enters this environment, and associates with one of these APs, they can locate the user in turn almost instantaneously relative to their own position.

In LocAP we have analyzed the 2D scenario when the access point is in the same plane as the user to be located. In a real world deployment the access point is placed at least a meter above the user height thus subtending a non-zero polar angle at the access point. This does not affect LocAP's algorithm on relative geometry prediction as the cartesian co-ordinates defined absorb the polar angular term. Thus unchanging the formulation of the relative antenna geometry prediction algorithm. Thus LocAP predicts the effective projection of the AP's relative geometry into the plane of user localization.

References

[1] Apple Maps. https://www.apple.com/ios/maps/.

[2] Bing Maps. www.bing.com/maps.

[3] Google Maps. www.maps.google.com.

[4] Open Street Map. www.openstreetmap.org.

[5] N. A. Alsindi, B. Alavi, and K. Pahlavan. Measurement and modeling of ultrawideband toa-based ranging in indoor multipath environments. *IEEE Transactions on Vehicular Technology*, 58(3):1046–1058, 2009.

[6] Apple. Airport Support.

[7] R. Ayyalasomayajula, D. Vasisht, and D. Bharadia. Bloc: Csi-based accurate localization for ble tags. In *Proceedings of the 14th International Conference on emerging Networking EXperiments and Technologies*, pages 126–138. ACM, 2018.

[8] V. Bahl and V. Padmanabhan. RADAR: An In-Building RF-based User Location and Tracking System. INFOCOM, 2000.

[9] BOSCH. Laser Measure DLE40 professional.

[10] M. Cao, B. D. Anderson, and A. S. Morse. Sensor network localization with imprecise distances. *Systems & control letters*, 55(11):887–893, 2006.

[11] Y.-T. Chan, W.-Y. Tsui, H.-C. So, and P.-c. Ching. Time-of-arrival based localization under nlos conditions. *IEEE Transactions on Vehicular Technology*, 55(1):17–24, 2006.

[12] H. Chen, G. Wang, Z. Wang, H.-C. So, and H. V. Poor. Non-line-of-sight node localization based on semi-definite programming in wireless sensor networks. *IEEE Transactions on Wireless Communications*, 11(1):108–116, 2012.

[13] K. Chintalapudi, A. Padmanabha Iyer, and V. N. Padmanabhan. Indoor Localization Without the Pain. MobiCom, 2010.

[14] S. Choi, Q.-Y. Zhou, and V. Koltun. Robust reconstruction of indoor scenes. In *Proceedings of the IEEE Conference on Computer Vision and Pattern Recognition*, pages 5556–5565, 2015.

[15] L. Cong and W. Zhuang. Nonline-of-sight error mitigation in mobile location. *IEEE Transactions on Wireless Communications*, 4(2):560–573, 2005.

[16] C. Di Franco, A. Prorok, N. Atanasov, B. Kempke, P. Dutta, V. Kumar, and G. J. Pappas. Calibration-free network localization using non-line-of-sight ultra-wideband measurements. In *Proceedings of the 16th ACM/IEEE International Conference on Information Processing in Sensor Networks*, pages 235–246. ACM, 2017.

[17] Y. Diao, Z. Lin, and M. Fu. A barycentric coordinate based distributed localization algorithm for sensor networks. *IEEE Transactions on Signal Processing*, 62(18):4760–4771, 2014.

[18] J. Gjengset, J. Xiong, G. McPhillips, and K. Jamieson. Phaser: Enabling Phased Array Signal Processing on Commodity Wi-Fi Access Points. *MobiCom*, 2014.

[19] A. Goswami, L. E. Ortiz, and S. R. Das. Wigem: A learning-based approach for indoor localization. In *Proceedings of the Seventh COnference on emerging Networking EXperiments and Technologies*, page 3. ACM, 2011.

[20] G. Grisetti, R. Kummerle, C. Stachniss, and W. Burgard. A tutorial on graph-based slam. *IEEE Intelligent Transportation Systems Magazine*, 2(4):31–43, 2010.

[21] G. Grisetti, C. Stachniss, W. Burgard, et al. Improved techniques for grid mapping with rao-blackwellized particle filters. *IEEE transactions on Robotics*, 23(1):34, 2007.

[22] D. Han, D. G. Andersen, M. Kaminsky, K. Papagiannaki, and S. Seshan. Access point localization using local signal strength gradient. In *International Conference on Passive and active network measurement*, pages 99–108. Springer, 2009.

[23] V. Ila, L. Polok, M. Solony, and P. Svoboda. Highly efficient compact pose slam with slam++. *arXiv preprint arXiv:1608.03037*, 2016.

[24] V. Iyer, V. Talla, B. Kellogg, S. Gollakota, and J. Smith. Inter-technology backscatter: Towards internet connectivity for implanted devices. In *SIGCOMM*, 2016.

[25] K. Joshi, S. Hong, and S. Katti. PinPoint: Localizing Interfering Radios. NSDI, 2013.

[26] M. Kaess and F. Dellaert. Covariance recovery from a square root information matrix for data association. *Robotics and autonomous systems*, 57(12):1198–1210, 2009.

[27] B. Kellogg, A. Parks, S. Gollakota, J. R. Smith, and D. Wetherall. Wi-fi backscatter: Internet connectivity for rf-powered devices. In *ACM SIGCOMM Computer Communication Review*, 2014.

[28] B. Kellogg, V. Talla, S. Gollakota, and J. R. Smith. Passive wi-fi: Bringing low power to wi-fi transmissions. In *NSDI*, 2016.

[29] B. Kempke, P. Pannuto, and P. Dutta. Harmonium: Asymmetric, bandstitched uwb for fast, accurate, and robust indoor localization. In *2016 15th ACM/IEEE International Conference on Information Processing in Sensor Networks (IPSN)*, pages 1–12. IEEE, 2016.

[30] U. A. Khan, S. Kar, and J. M. Moura. Distributed sensor localization in random environments using minimal number of anchor nodes. *IEEE Transactions on Signal Processing*, 57(5):2000–2016, 2009.

[31] U. A. Khan, S. Kar, and J. M. Moura. Diland: An algorithm for distributed sensor localization with noisy distance measurements. *IEEE Transactions on Signal Processing*, 58(3):1940–1947, 2010.

[32] M. Kotaru, K. Joshi, D. Bharadia, and S. Katti. SpotFi: Decimeter Level Localization Using Wi-Fi. SIGCOMM, 2015.

[33] M. Kotaru and S. Katti. Position tracking for virtual reality using commodity wifi. In *Proceedings of the IEEE Conference on Computer Vision and Pattern Recognition*, pages 68–78, 2017.

[34] S. Kumar, S. Gil, D. Katabi, and D. Rus. Accurate Indoor Localization with Zero Start-up Cost. MobiCom, 2014.

[35] M. Labbe and F. Michaud. Rtab-map as an open-source lidar and visual simultaneous localization and mapping library for large-scale and long-term online operation. *Journal of Field Robotics*, 2019.

[36] A. M. Ladd, K. E. Bekris, A. Rudys, L. E. Kavraki, and D. S. Wallach. Robotics-based location sensing using wireless ethernet. *Wireless Networks*, 11(1-2):189–204, 2005.

[37] Y. Ma, N. Selby, and F. Adib. Drone relays for battery-free networks. In *SIGCOMM*.

[38] A. T. Mariakakis, S. Sen, J. Lee, and K.-H. Kim. Sail: Single access point-based indoor localization. In *Proceedings of the 12th annual international conference on Mobile systems, applications, and services*, pages 315–328. ACM, 2014.

[39] J. Neira and J. D. Tardós. Data association in stochastic mapping using the joint compatibility test. *IEEE Transactions on robotics and automation*, 17(6):890–897, 2001.

[40] N. B. Priyantha, A. Chakraborty, and H. Balakrishnan. The cricket location-support system. In *Proceedings of the 6th annual international conference on Mobile computing and networking*, pages 32–43. ACM, 2000.

[41] A. Prorok and A. Martinoli. Accurate indoor localization with ultra-wideband using spatial models and collaboration. *The International Journal of Robotics Research*, 33(4):547–568, 2014.

[42] Quantenna. Quantenna 802.11ac WiFi Card.

[43] Z. Sahinoglu. *Ultra-wideband positioning systems*. Cambridge university press, 2008.

[44] S. Sen, J. Lee, K.-H. Kim, and P. Congdon. Avoiding multipath to revive inbuilding wifi localization. In *Proceeding of the 11th annual international conference on Mobile systems, applications, and services*, pages 249–262. ACM, 2013.

[45] S. Sen, B. Radunovic, R. R. Choudhury, and T. Minka. You are facing the mona lisa: Spot localization using phy layer information. In *Proceedings of the 10th international conference on Mobile systems, applications, and services*, pages 183–196. ACM, 2012.

[46] E. Soltanaghaei, A. Kalyanaraman, and K. Whitehouse. Multipath triangulation: Decimeter-level wifi localization and orientation with a single unaided receiver. In *MobiSyS*, 2018.

[47] A. P. Subramanian, P. Deshpande, J. Gao, and S. R. Das. Drive-by localization of roadside wifi networks. In *IEEE INFOCOM 2008-The 27th Conference on Computer Communications*, pages 718–725. IEEE, 2008.

[48] T-Series. VICON. www.vicon.com/products/documents/Tseries.pdf.

[49] G. D. Tipaldi, G. Grisetti, and W. Burgard. Approximate covariance estimation in graphical approaches to slam. In *2007 IEEE/RSJ International Conference on Intelligent Robots and Systems*, pages 3460–3465. IEEE, 2007.

[50] Tutlebot. Turtlebot Robotics.

[51] M. C. Vanderveen, C. B. Papadias, and A. Paulraj. Joint angle and delay estimation (jade) for multipath signals arriving at an antenna array. *IEEE Communications letters*, 1(1):12–14, 1997.

[52] D. Vasisht, S. Kumar, and D. Katabi. Decimeter-Level Localization with a Single Wi-Fi Access Point. NSDI, 2016.

[53] J. Wang, F. Adib, R. Knepper, D. Katabi, and D. Rus. Rf-compass: Robot object manipulation using rfids. In *Proceedings of the 19th annual international conference on Mobile computing & networking*, pages 3–14. ACM, 2013.

[54] J. Wang, F. Adib, R. Knepper, D. Katabi, and D. Rus. RF-compass: Robot Object Manipulation Using RFIDs. MobiCom, 2013.

[55] J. Wang, H. Jiang, J. Xiong, K. Jamieson, X. Chen, D. Fang, and B. Xie. LiFS: Low Human-effort, Device-free Localization with Fine-grained Subcarrier Information. MobiCom, 2016.

[56] J. Wang, D. Vasisht, and D. Katabi. Rf-idraw: Virtual touch screen in the air using rf signals. *ACM SIGCOMM*, 2014.

[57] Y. Xie, J. Xiong, M. Li, and K. Jamieson. xd-track: leveraging multi-dimensional information for passive wi-fi tracking. In *HotWireless*, pages 39–43. ACM, 2016.

[58] Y. Xie, J. Xiong, M. Li, and K. Jamieson. md-track: Leveraging multi-dimensionality in passive indoor wi-fi tracking. *arXiv preprint arXiv:1812.03103*, 2018.

[59] J. Xiong and K. Jamieson. ArrayTrack: A Fine-grained Indoor Location System. NSDI, 2013.

[60] J. Xiong, K. Jamieson, and K. Sundaresan. Synchronicity: Pushing the envelope of fine-grained localization with distributed mimo. In *HotWireless*, 2014.

[61] J. Xiong, K. Sundaresan, and K. Jamieson. ToneTrack: Leveraging Frequency-Agile Radios for Time-Based Indoor Wireless Localization. MobiCom , 2015.

[62] C. Xu, B. Firner, Y. Zhang, R. Howard, J. Li, and X. Lin. Improving RF-based Device-free Passive Localization in Cluttered Indoor Environments Through Probabilistic Classification Methods. IPSN, 2012.

[63] L. Yang, Y. Chen, X.-Y. Li, C. Xiao, M. Li, and Y. Liu. Tagoram: Real-time tracking of mobile rfid tags to high precision using cots devices. MobiCom, 2014.

[64] M. Youssef and A. Agrawala. The Horus WLAN Location Determination System. MobiSys, 2005.

[65] P. Zhang, D. Bharadia, K. Joshi, and S. Katti. Hitchhike: Practical backscatter using commodity wifi. In *SenSys*, 2016.

[66] X. Zhu and Y. Feng. Rssi-based algorithm for indoor localization. *Communications and Network*, 5(02):37, 2013.